

Lateral Torsional Buckling of Steel I-Beams in Case of Fire – Numerical Modelling

Paulo M. M. Vila Real * ; Jean-Marc Franssen **

* Departamento de Engenharia Civil, Universidade de Aveiro – Campus Santiago - 3810 Aveiro, Portugal
(email: pvreal@civil.ua.pt, tel: 351-34-370049)

** Institut de Mécanique et Génie Civil - Service "Ponts et Charpentes", Université de Liège – Chemin des Chevreuils, 1 - B
4000 Liège 1, Belgium
(email: JM.franssen@ulg.ac.be, tel: 32-4-3669251)

ABSTRACT

A geometrically and materially non-linear finite element program, i. e., a general model, has been used to determine the lateral-torsional resistance of steel I-beams under fire conditions, according to the hypotheses of Eurocode 3, Part 1-2. Two yield strengths, one cross section, one type of load and four durations of exposure to the ISO834 standard fire have been considered. The numerical results have been compared to the simple models presented in Eurocode 3, Part 1-2. These simple models lead to a safety level that depends on the slenderness of the beam, being unsafe for intermediate non-dimensional slenderness when compared with the general model. A new proposal has been made for a simple model that ensures a conservative result when compared to the general model.

1. INTRODUCTION

Although the problem of lateral buckling of steel beams at room temperature is well known [12], the same problem at elevated temperature is not. Among the work done in this field there is the paper from Bailey et al. [16] who uses a three-dimensional computer model to investigate the ultimate behaviour of uniformly heated unrestrained beams. In this paper, a simple model for fire resistance of lateral-torsional buckling of steel I-beams is presented. It is based on the numerical results of the SAFIR program, a geometrically and materially non-linear code specially established for the analysis of structures submitted to the fire [3]. The capability of this code to model the lateral buckling of beams has been demonstrated [11] at room temperature by comparisons with the formulas of Eurocode 3, Part 1-1 [1].

It has been used a three-dimensional (3D) beam element based on the following formulations and hypotheses:

- Displacement type element in a total corrotational description;
- Prismatic element;
- The displacement of the node line is described by the displacements of the three nodes of the element, two nodes at each ends supporting seven degree of freedom, three translations, three rotations and the warping amplitude plus one node at mid-length supporting one degree of freedom, the non-linear part of the longitudinal displacement;
- The Bernoulli hypothesis is considered, i. e., plane sections remain plane and perpendicular to the longitudinal axis and no shear energy is considered;
- No local buckling is taken into account, reason why the proposal in this paper is valid only for Class 1 and Class 2 sections [1];
- The strains are small (von Kármán hypothesis), i. e.

$$\frac{1}{2} \frac{\partial u}{\partial x} \ll 1$$

where u is the longitudinal displacement and x is the longitudinal co-ordinate;

- The angles between the deformed longitudinal axis and the undeformed but translated longitudinal axis are small, i. e.,

$$\sin \varphi \cong \varphi \text{ and } \cos \varphi \cong 1$$

where φ is the angle between the arc and the cord of the beam finite element.

- The longitudinal integrations are numerically calculated using Gauss' method;
- The cross-section is discretised by means of triangular or quadrilateral fibers. At every longitudinal point of integration, all variables, such as temperature, strain, stress, etc., are uniform in each fiber;
- The tangent stiffness matrix is evaluated at each iteration of the convergence process (pure Newton-Raphson method);
- Residual stresses are considered by means of initial, and constant, strains [14];
- The material behaviour in case of strain unloading is elastic, with the elastic modulus equal to the Young's modulus at the origin of the stress-strain curve. In one cross section, some fibers that have yielded may therefor exhibit a decreased tangent modulus because they are still on the loading branch, whereas, at the same time, some other fibers behave elastically. The plastic strain is presumed not to be affected by a change in temperature [15].

A simply supported steel beam described in [11] has been studied to compare the results between the EUROCODE 3, Part 1-2 [2] and the SAFIR code under fire conditions.

It has been assumed that the beam had a geometrical imperfection of sinusoidal type [4-6] and residual stresses [7] were considered.

The beam has been submitted to a uniform moment (see Figure 1) and has ends that cannot deflect laterally or twist (but are provided with no other restraining effects).

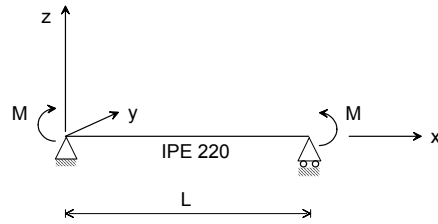


Fig. 1 – Simply supported beam submitted to moments at the ends.

The results of the Eurocode 3 and the SAFIR code were compared for the unprotected beam after 10, 15, 20 and 30 minutes of exposure to the ISO834 standard fire.

2. LATERAL-TORSIONAL BUCKLING UNDER FIRE CONDITIONS

2.1 Analysis according to the Eurocode 3

The temperature of the beam after the desired time has been obtained using the simplified equation of Eurocode 3 Part 1.2 [2]. From this temperature (which is uniform in the beam cross section), the buckling resistance moment $M_{b,fi,t,Rd}$ at time t , provided that the non-dimensional slenderness $\bar{\lambda}_{LT,\theta,com}$ for the maximum temperature in the compression flange $\theta_{a,com}$ reached at time t exceeds the value of 0.4, has been determined according to:

$$M_{b,fi,t,Rd} = \frac{\chi_{LT,fi}}{1.2} w_{pl,y} k_{y,\theta,com} f_y \frac{1}{\gamma_{M,fi}} \quad (1)$$

where:

- $\chi_{LT,fi}$ is the reduction factor for lateral-torsional buckling in the fire design situation;
- $w_{pl,y}$ is the plastic section modulus;
- $k_{y,\theta,com}$ is the reduction factor for the yield strength at the maximum temperature in the compression flange $\theta_{a,com}$, reached at time t (see Figure 2, a);
- $\gamma_{M,fi}$ is the partial safety factor for the fire situation (usually $\gamma_{M,fi} = 1$).

The constant 1.2 is an empirically determined value and is used as a correction factor that allows for a number of effects.

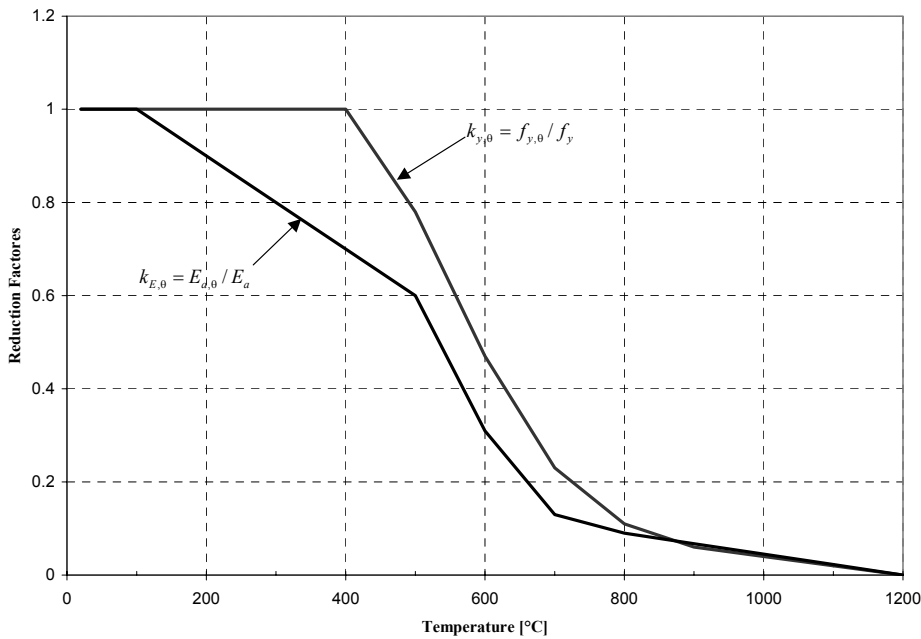
The reduction factor for lateral-torsional buckling in fire design situation, $\chi_{LT,fi}$, must be determined as for room temperature case, except using the non-dimensional slenderness $\bar{\lambda}_{LT,\theta,com}$ for temperature $\theta_{a,com}$ given by

$$\bar{\lambda}_{LT,\theta,com} = \bar{\lambda}_{LT} \sqrt{\frac{k_{y,\theta,com}}{k_{E,\theta,com}}} \quad (2)$$

where

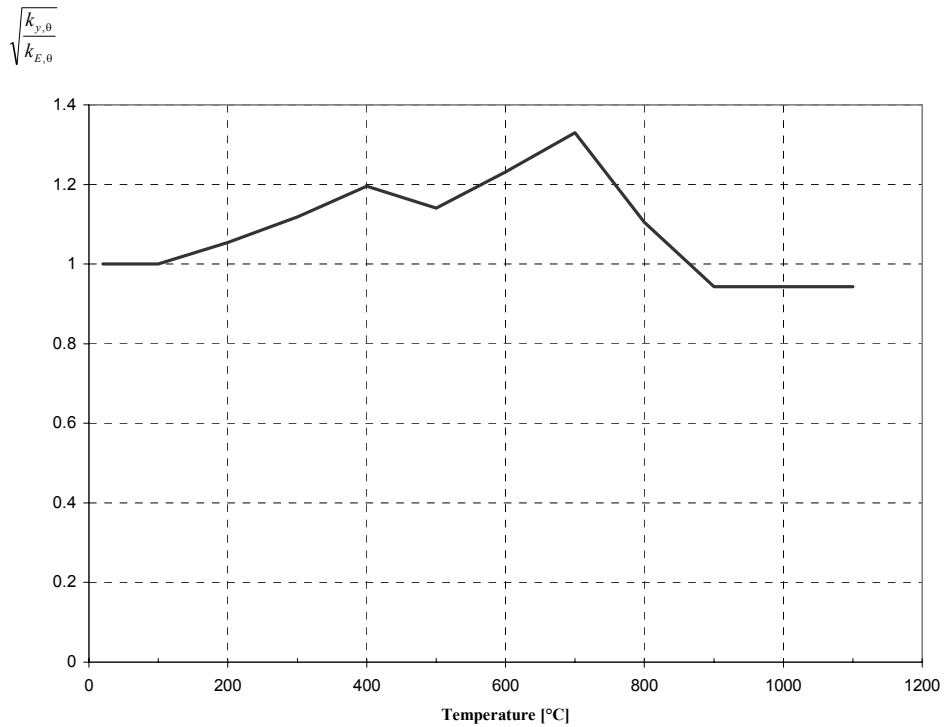
$\bar{\lambda}_{LT}$ is the non-dimensional slenderness at room temperature;
 $k_{E,\theta,com}$ is the reduction factor for the slope of the linear elastic range at the maximum steel temperature in the compression flange $\theta_{a,com}$ reached at time t (see Figure 2, a).

The factor $\sqrt{k_{y,\theta,com} / k_{E,\theta,com}}$, which is represented in Figure 2, b), leads to a particular behaviour of the non-dimensional slenderness $\bar{\lambda}_{LT,\theta,com}$. It could be expected that this slenderness should increase with the temperature but, according to the Eurocode 3 material model, this is not the case as it can be seen in Figure 3. In that figure is represented the variation of the non-dimensional slenderness, $\bar{\lambda}_{LT,\theta,com}$, with the temperature, for the Fe 360 and Fe 510 steel and for a IPE 220 beam with 2.0 meters span.



a) Reduction factors $k_{y,\theta,com}$ and $k_{E,\theta,com}$

Fig. 2 – Dependency with temperature.



b) Factor $\sqrt{k_{y,\theta,com} / k_{E,\theta,com}}$

Fig. 2 – Dependency with temperature (cont.).

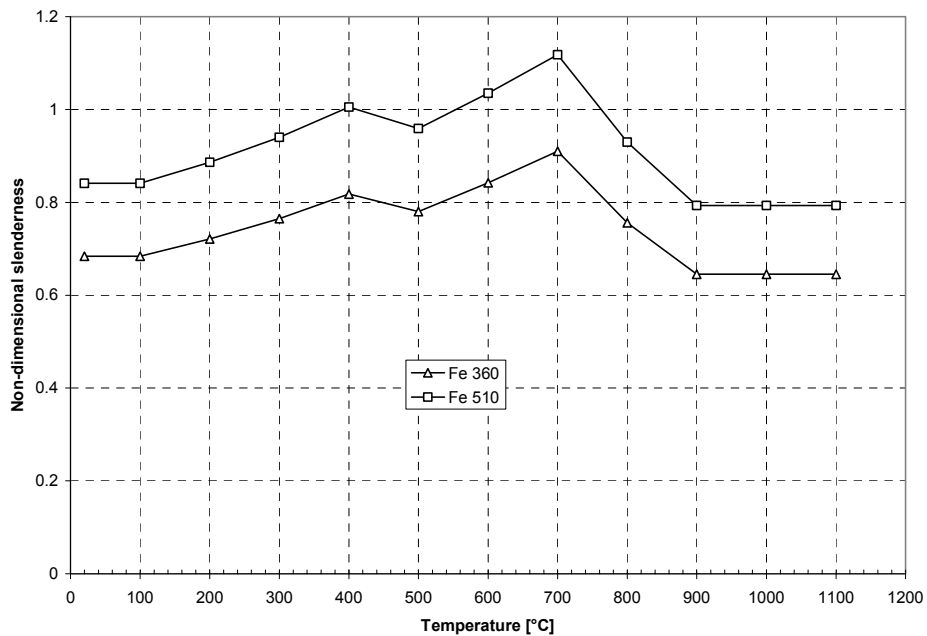


Fig. 3 – Dependency of the non-dimensional slenderness with temperature for a IPE 220 beam with 2 meters span.

Figure 4 shows the variation with the temperature of the length of a IPE 220 simply supported beam that corresponds to a non-dimensional slenderness of 0.4. As it can be seen this length is shorter than the length at room temperature for temperatures between 100 °C

and approximately 850 °C for the two types of steel. This is also due to the Eurocode 3, Part 1-2, material model.

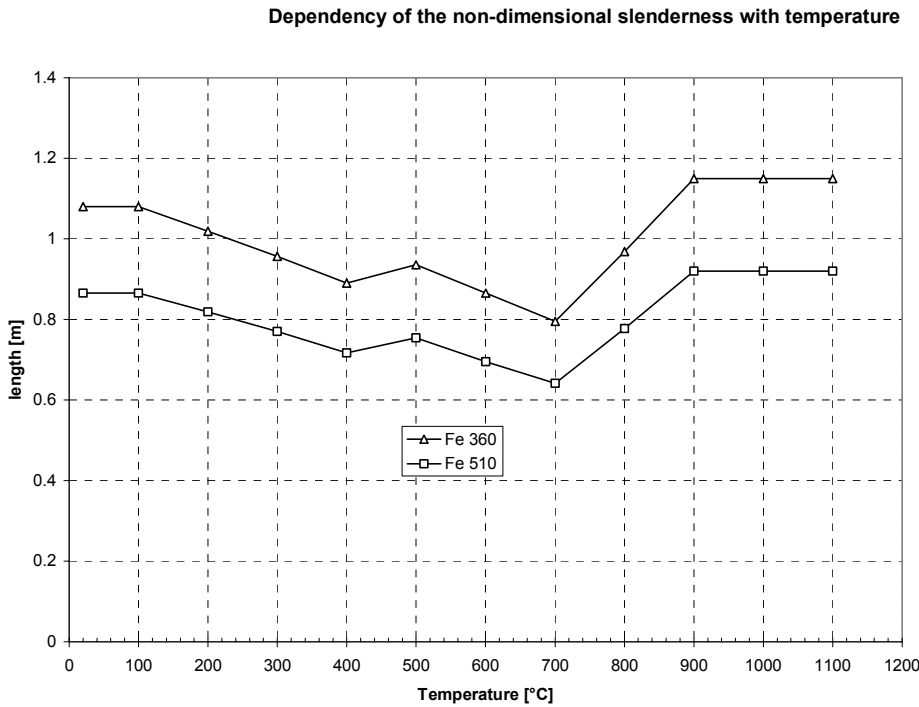


Fig. 4 – Dependency of the length of a IPE 220 simply supported beam corresponding to $\lambda_{LT,\theta,com} = 0.4$ with the temperature.

The full line of Figure 5 shows the beam design curve of Eurocode 3. For all the temperatures greater than 20 °C this curve is unique and named EC3,fi in that figure. On the vertical axis is the ratio

$$\frac{M_{b,fi,t,Rd}}{M_{fi,\theta,Rd}} \quad (3)$$

where, $M_{b,fi,t,Rd}$ is the design lateral buckling resistance moment at time t of a laterally unrestrained beam given by equation (1) and the design moment resistance $M_{fi,\theta,Rd}$ of a Class 1 or 2 cross-section with a uniform temperature θ_a may be determined from:

$$M_{fi,\theta,Rd} = k_{y,\theta} \frac{\gamma_{M0}}{\gamma_{M,fi}} M_{Rd} \quad (4)$$

where, $\gamma_{M0} = 1.0$, $\gamma_{M,fi} = 1.0$ and M_{Rd} is the plastic resistance of the gross cross-section $M_{pl,Rd}$ for normal temperature, which is given by

$$M_{Rd} = \frac{w_{pl,y} f_y}{\gamma_{M0}} \quad (5)$$

where $\gamma_{M0} = 1.0$.

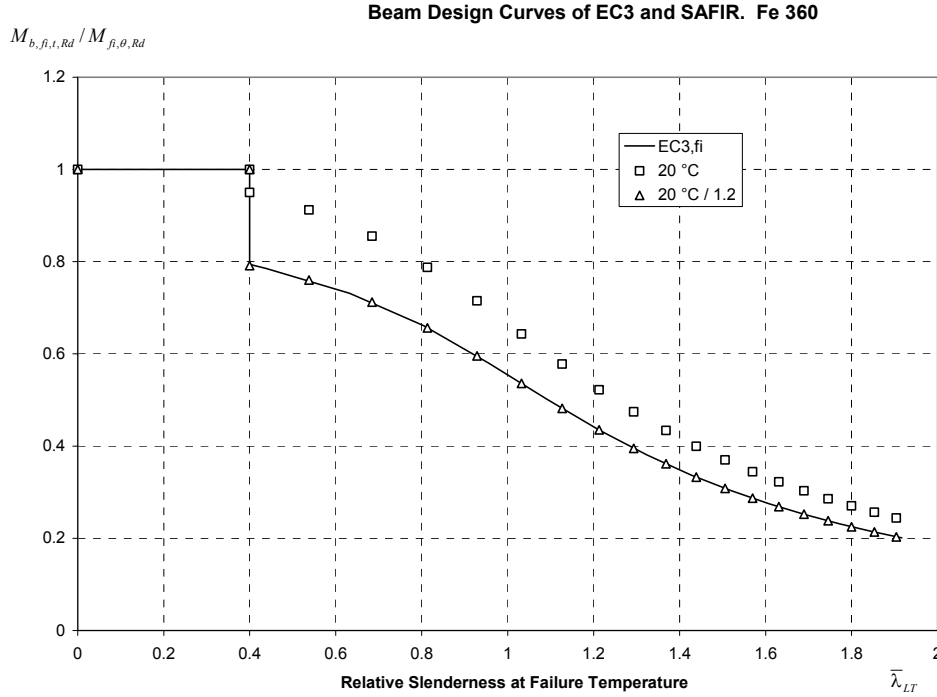


Fig. 5 – Beam design curve of Eurocode 3 for fire situation (EC3,fi) and at room temperature (20°C).

In that figure, it can also be seen that the buckling design curve at 20 °C is different from the curve at elevated temperature due to the empirical factor 1.2. This figure shows that the curve at elevated temperature, EC3,fi, is the curve at 20 °C divided by 1.2.

So it must be emphasised that in the beam design curves used throughout this paper the ratio $M_{b,fi,t,Rd} / M_{fi,\theta,Rd}$ plotted on the vertical axis represents the reduction factor for lateral-torsional buckling in the fire design situation $\chi_{LT,fi}$ divided by 1.2, i. e.:

$$\frac{M_{b,fi,t,Rd}}{M_{fi,\theta,Rd}} = \frac{\chi_{LT,fi}}{1.2}, \text{ for the Eurocode 3, Part 1-2 results} \quad (6.a)$$

or

$$\frac{M_{SAFIR}}{M_{fi,\theta,Rd}}, \text{ for the SAFIR results} \quad (6.b)$$

It must also be mentioned that the Class of cross-section of the IPE 220 was checked for all the analysed temperatures to see if it maintains as a Class1 cross-section like at room temperature [8] or not. This was done using the modified value of ε given by [2]:

$$\varepsilon = [(235 / f_y)(k_{E,\theta} / k_{y,\theta})]^{0.5} \quad (7)$$

It has been concluded that the Class of the cross-section doesn't change with the temperature.

2.2 Analysis with the SAFIR code

The time evolution of the temperature is obtained using finite element analysis. So the temperature field is not uniform like the one obtained with the simplified equation of Eurocode 3, see Figure 6

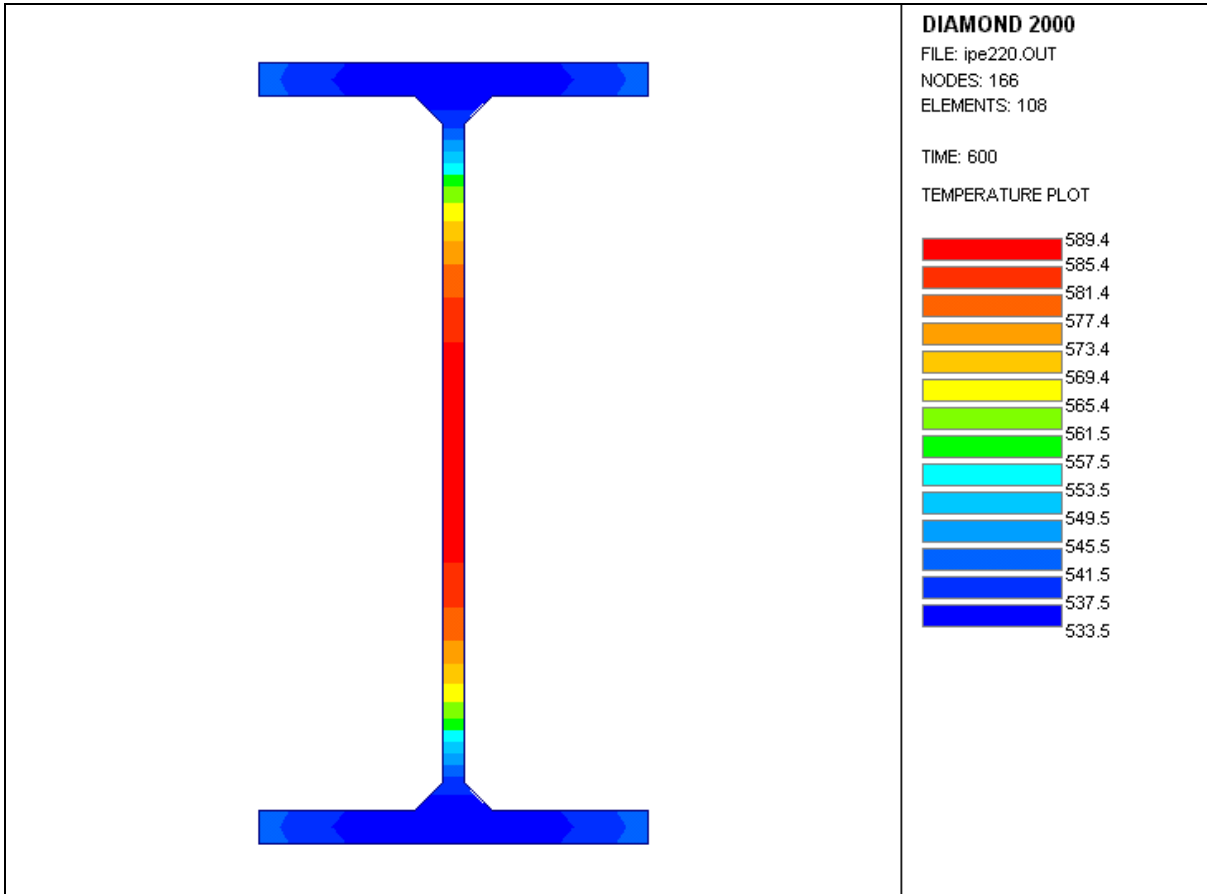


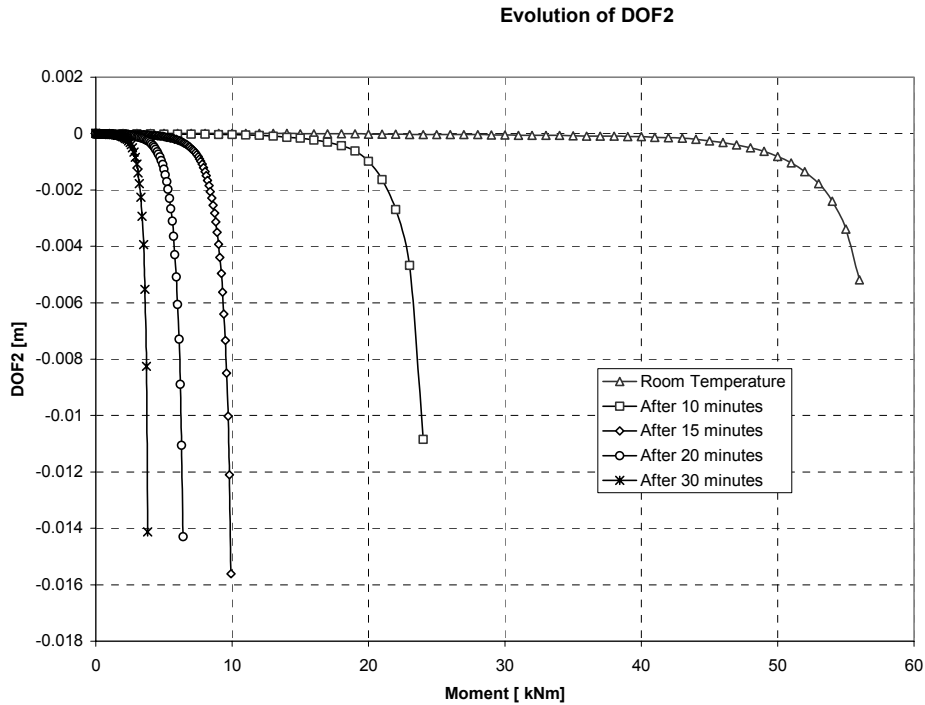
Fig. 6 – Temperature field after 10 minutes, obtained with SAFIR.

For the temperature reached at time t (10,15,20 and 30 minutes) the load was applied with step increments of 100 Nm (for the temperature at 10, 15 and 20 minutes) or 50 Nm (for the temperature at 30 minutes).

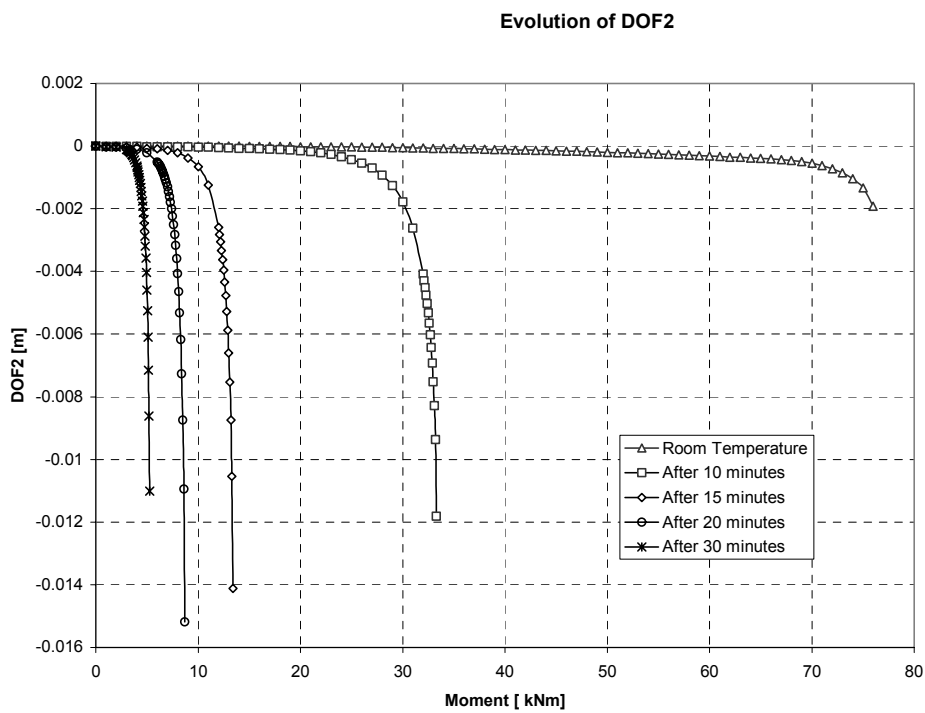
The numerical simulations were carried out considering the following assumptions:

- End conditions: ends that cannot deflect laterally or twist but are provided with no other restraining effects;
- Beam lateral imperfection: Sinusoidal, with a maximum value of $L/1000$;
- Longitudinal integration: two Gauss points;
- Residual stresses: constant across the thickness of the web and of the flanges. Triangular distribution with a maximum value of 0.3×235 Mpa [7], for the Fe 360 steel as well as for the Fe 510 steel.

Figures 7, 8 and 9 show for the IPE 220 beam with 2 meters span, the evolution of the vertical and lateral displacement and the rotation around the longitudinal axis of the central node of the beam, with the increasing load for the time instant of 10, 15, 20 and 30 minutes.

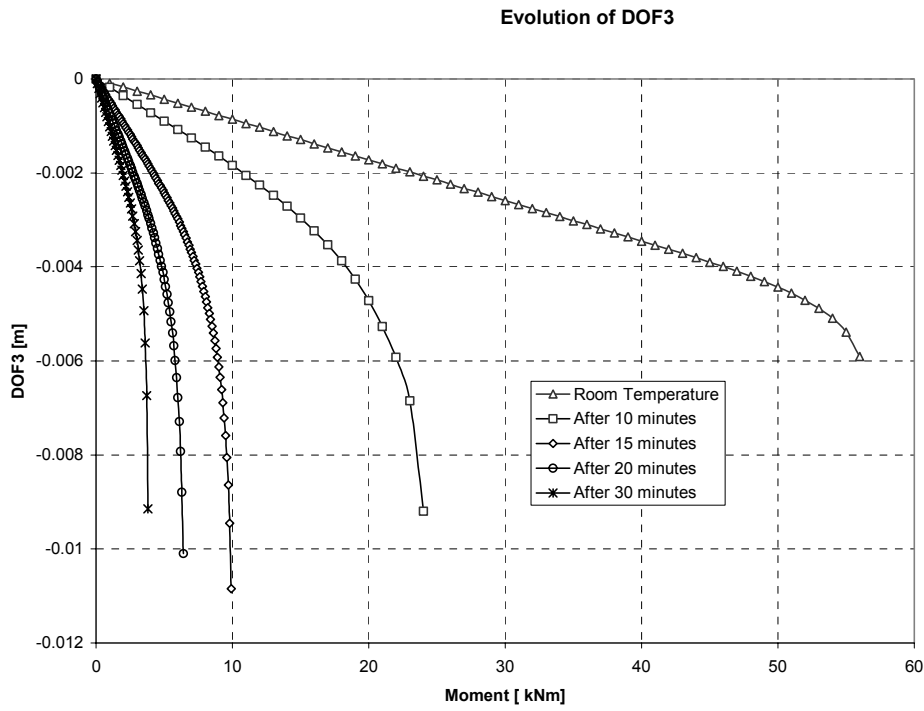


a) Fe 360 steel

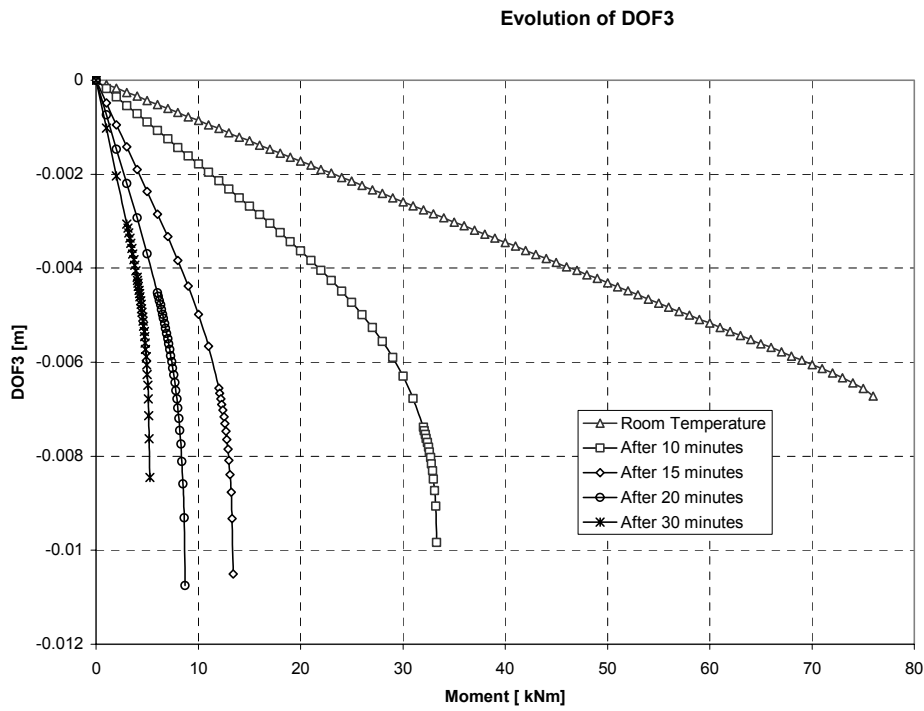


b) Fe 510

Fig. 7 – Evolution of the lateral displacement of the central node of a 2 meters span beam.

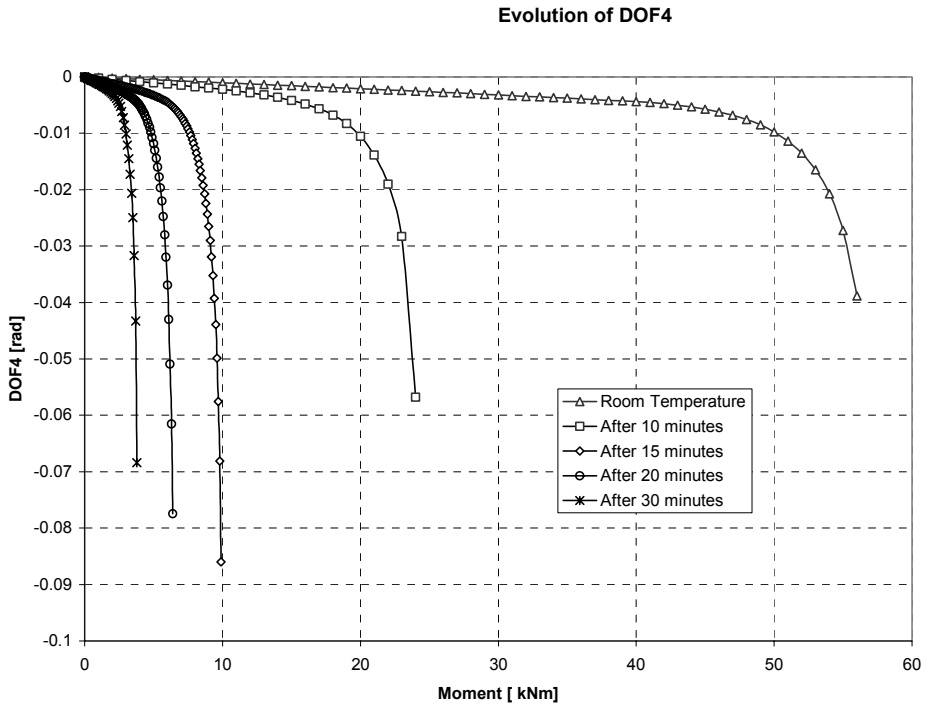


a) Fe 360 steel

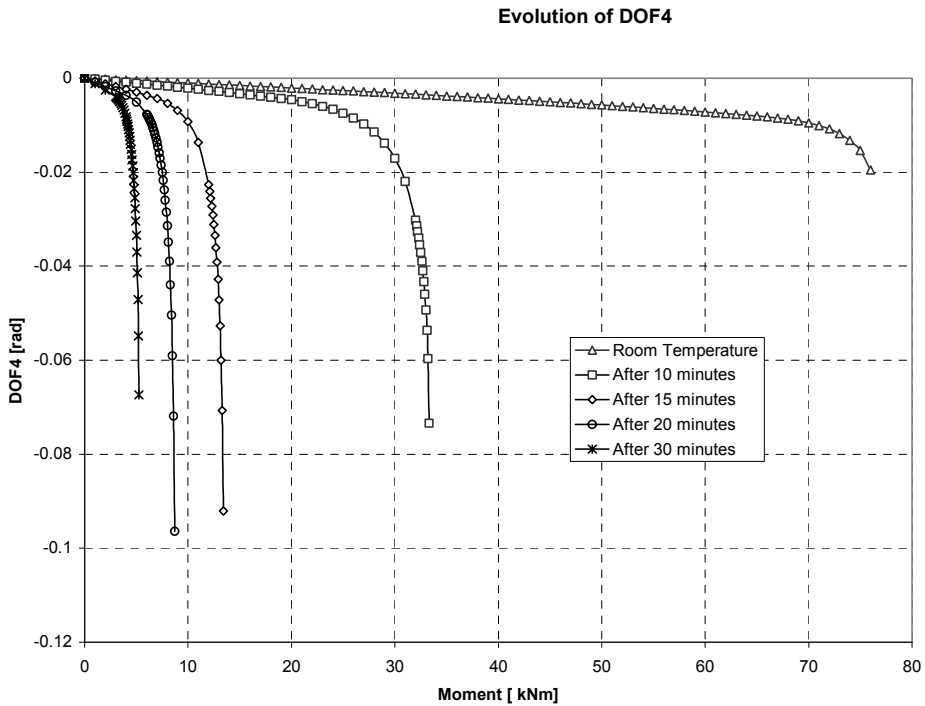


b) Fe 510

Fig. 8 – Evolution of the vertical displacement of the central node of a 2 meters span beam.



a) Fe 360 steel



b) Fe 510

Fig. 9 – Evolution of the longitudinal rotation of the central node of a 2 meters span beam.

The beam design curves for all the time instants studied are shown in Figures 10 to 13 for the Fe 360 and Fe510 steel. In these figures, $M_{b,fi,t,Rd}$ is the design lateral buckling resistance moment at time t of a laterally unrestrained beam given by equation (1) or

calculated by the SAFIR code and the design moment resistance $M_{fi,\theta,Rd}$ of a Class 1 or 2 cross-section is given by equation (4) evaluated for the temperatures obtained with the simplified equation of the Eurocode 3, i. e., 554 °C, 680 °C, 733 °C and 827 °C for the time instants 10, 15, 20 and 30 minutes respectively. The relative slenderness was calculated at failure temperature according to equation (2).

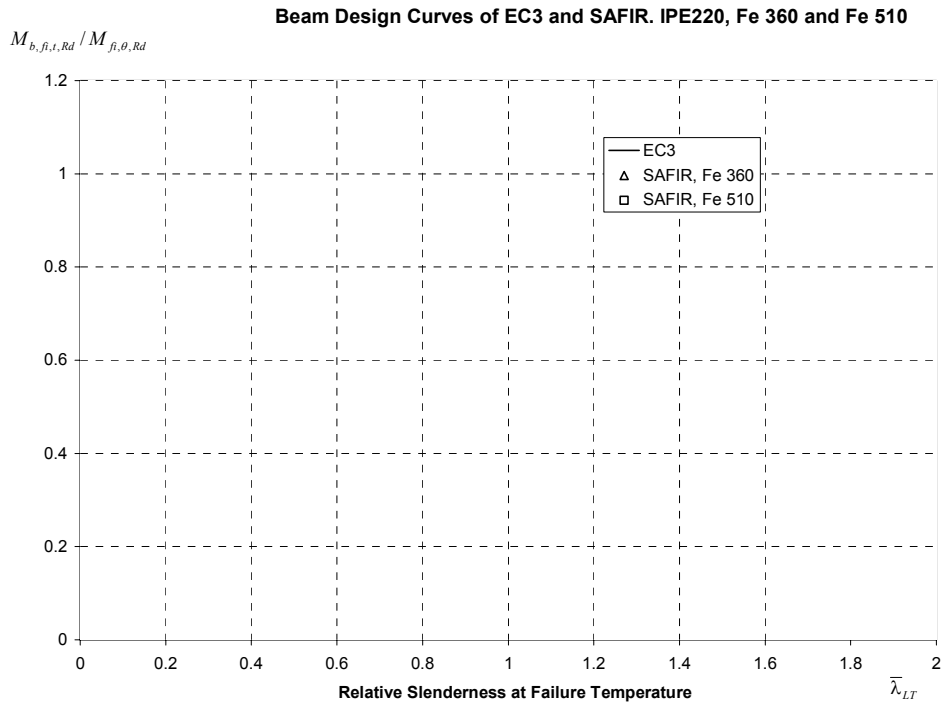


Fig. 10 – Beam design curve after 10 minutes. Comparison between the Eurocode 3 and SAFIR, for Fe 360 and Fe 510 steel.

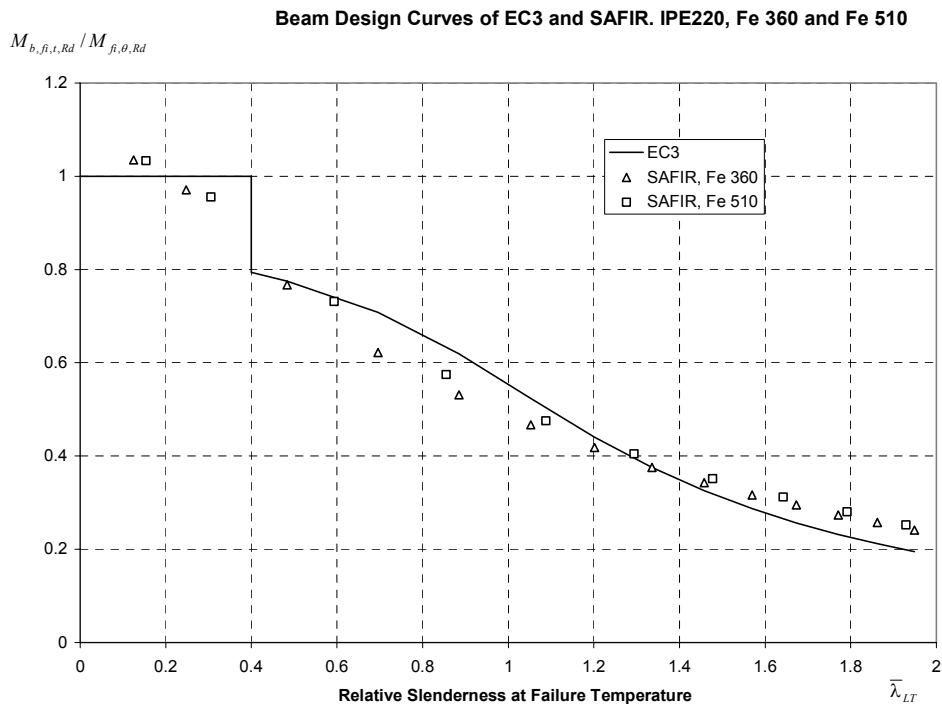


Fig. 11 – Beam design curve after 15 minutes. Comparison between the Eurocode 3 and SAFIR, for Fe 360 and Fe 510 steel.

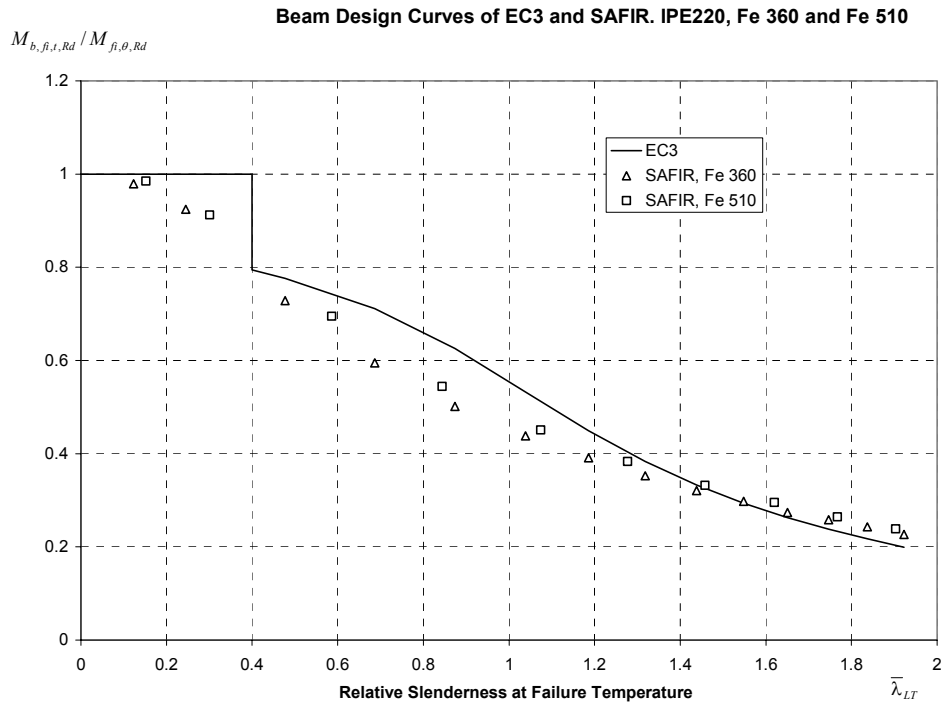


Fig. 12 – Beam design curve after 20 minutes. Comparison between the Eurocode 3 and SAFIR, for Fe 360 and Fe 510 steel.

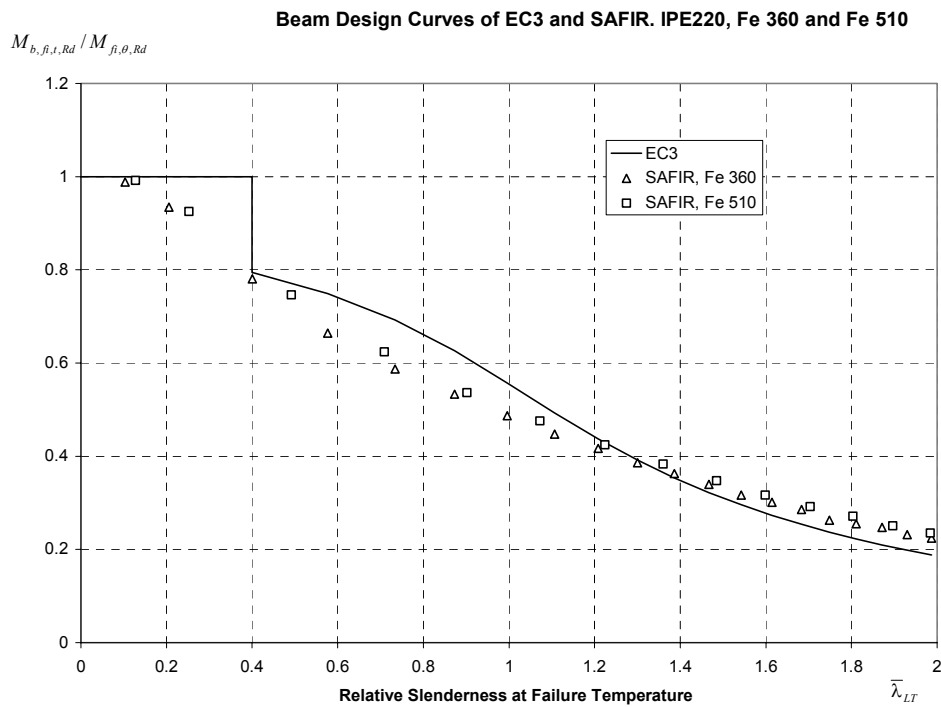
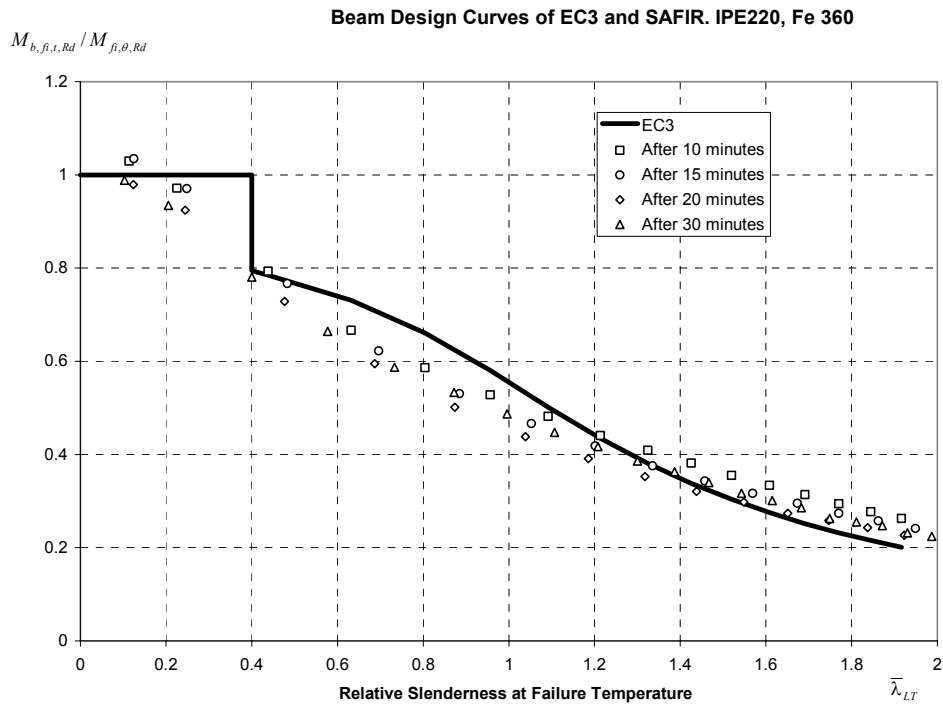
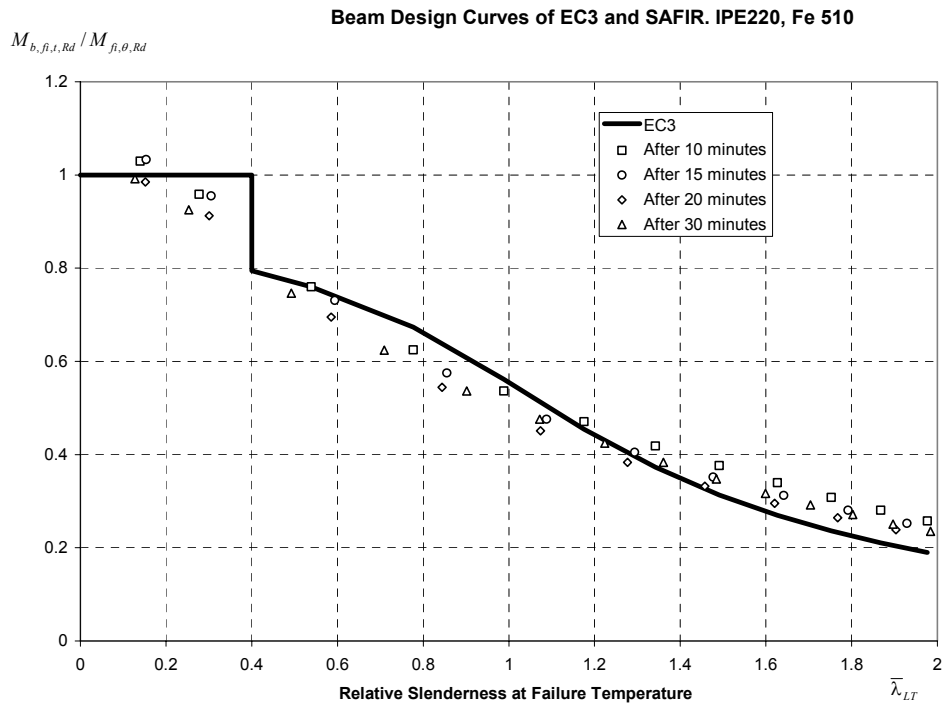


Fig. 13 – Beam design curve after 30 minutes. Comparison between the Eurocode 3 and SAFIR, for Fe 360 and Fe 510 steel.

Figure 14 shows the beam design curve obtained with the SAFIR results for the time instants of 10, 15, 20 and 30 minutes, all plotted at the same chart for the Fe 360 and Fe 510 steel. This curves are not coincident like in the case of the Eurocode 3 curve at elevated temperature (see for instance curve EC3,fi in Figure 5, or curve EC3 in Figures 10 to 13).



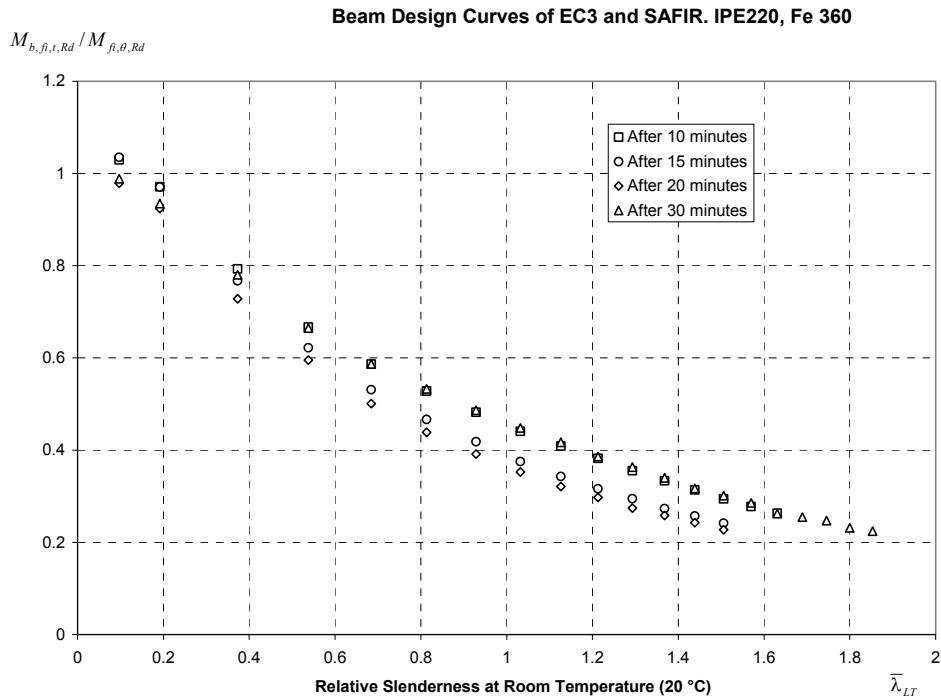
a) Fe 360 steel



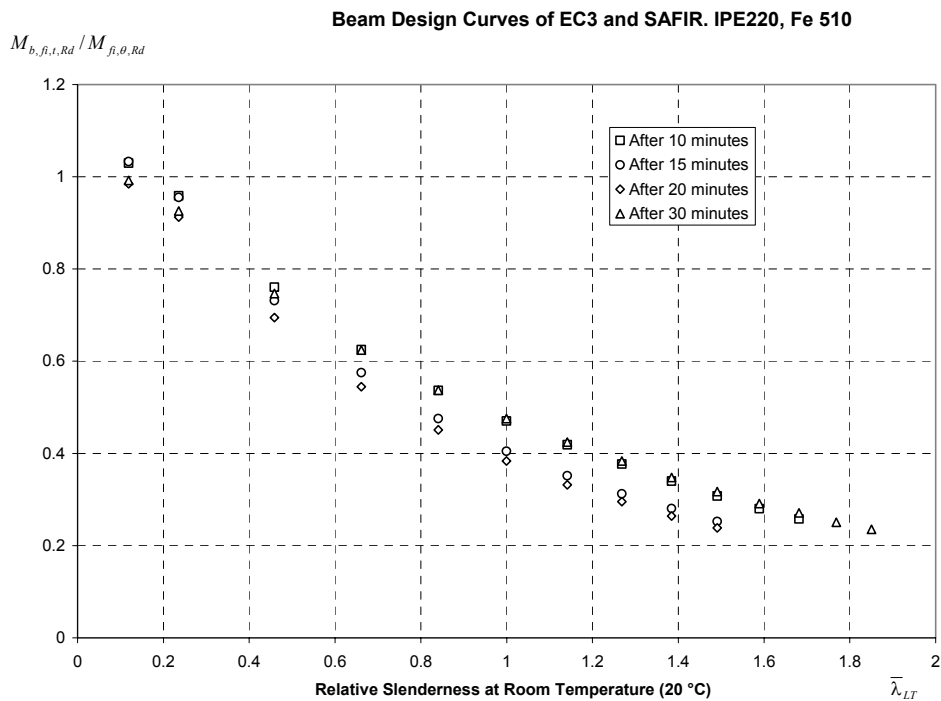
b) Fe 510

Fig. 14 – Beam design curve obtained with Eurocode 3 and SAFIR (after 10, 15, 20 and 30 minutes).

Until now all the charts were plotted with relative slenderness calculated at ultimate temperature. Figure 15 shows the numerical lateral-torsional buckling values using for the figure the relative slenderness at room temperature, i. e., at 20 °C.



a) Fe 360 steel



b) Fe 510

Fig. 15 – Beam design curve obtained with Eurocode 3 and SAFIR (after 10, 15, 20 and 30 minutes), using the relative slenderness evaluated at room temperature.

In Figures 10 to 14 all the named EC3 curves corresponds to the buckling curve c of the Eurocode 3, Part 1-1 [1], for $\bar{\lambda}_{LT} > 0.4$ divided by 1.2. The only difference between the numerical values in Figures 10 to 14 and the values in Figure 15 is that the variable on the horizontal axis of the diagrams is evaluated in the first case at ultimate temperature and in the last case at room temperature.

Anyway the shape of the distribution of the numerical lateral-torsional buckling curves is too different from the shape of the present analytical curve of Eurocode 3 to allow any hope that a modification of the correction factor used in the simple model could lead to a better correlation [6]. The lateral-torsional curve's distribution is thinner in Figure 14 than it is in Figure 15. This means that there is a better possibility of representing the numerical results, without excessive safety, with an analytical expression when the relative slenderness is evaluated at elevated temperature [6] than if it is evaluated at 20 °C. This is what will be done in the new proposal presented in the point 3 of this paper.

From Figure 10 to Figure 14 it can be seen that the numerical values are higher on the vertical axis for Fe 510 than they are for Fe 360. As stated in [6], "This is due to the fact that the residual stresses do not depend on the yield strength. Their relative influence is therefore smaller when the yield strength is increased. This phenomena is not accounted for in the simplified model of ref. [2], where the buckling coefficient does not vary with the yield strength". In fact the reduction factor for lateral-torsional buckling, χ_{LT} , depends on the yield strength as well as the non-dimensional slenderness, $\bar{\lambda}_{LT}$, but the lateral-torsional buckling curves do not depend on the yield strength.

The reason why in the Figures 10, 11 and 14 the ratio $M_{SAFIR} / M_{f_i,0,Rd}$, for low values of the slenderness and for the time instants 10 and 15 minutes, is greater than 1 is due to the fact that the temperature field obtained with SAFIR is not uniform, with temperatures in the flanges lower than the uniform temperature given by the simplified equation of the Eurocode 3 used to calculate $M_{f_i,0,Rd}$, see Figure 6 for the temperature field after 10 minutes. The uniform temperature after 10 minutes calculated with the Eurocode 3 is 554 °C, which is higher than the temperature in the flanges calculated with SAFIR. For longer duration, this effect tends to disappear because the temperature field becomes more and more uniform as can be seen in Figure 16, which shows the temperature field after 30 minutes obtained by finite elements using the SAFIR code. After 30 minutes the uniform temperature field obtained with the simplified equation of the Eurocode 3 is 827 °C. The maximum temperature difference after 30 minutes, for the SAFIR results, is only 11.9 °C (see Figure 16), while after 10 minutes it is 55.9 °C (see Figure 6).

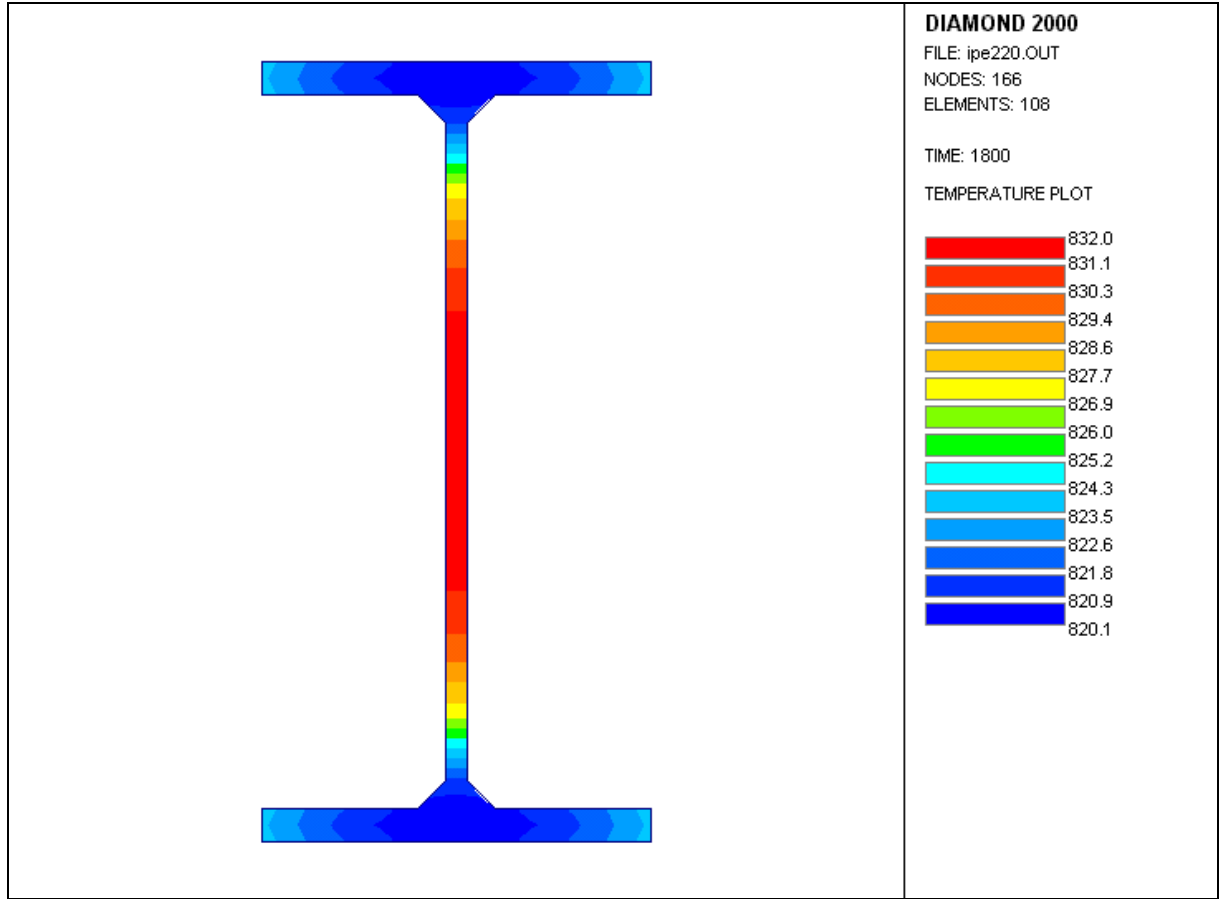


Fig. 16 – Temperature field after 30 minutes, obtained with SAFIR.

3. NEW PROPOSAL

Adopting the same proposal as in Franssen et al. [6] our approach to a new proposal is given bellow. The lateral-torsional buckling resistance moment is

$$M_{b,fi,t,Rd} = \chi_{LT,fi} W_{pl,y} k_{y,\theta,com} f_y \frac{1}{\gamma_{M,fi}} \quad (8)$$

where

$$\chi_{LT,fi} = \frac{1}{\phi_{LT,\theta,com} + \sqrt{[\phi_{LT,\theta,com}]^2 - [\bar{\lambda}_{LT,\theta,com}]^2}} \quad (9)$$

$$\phi_{LT,\theta,com} = \frac{1}{2} [1 + \alpha \bar{\lambda}_{LT,\theta,com} + (\bar{\lambda}_{LT,\theta,com})^2] \quad (10)$$

and

$$\bar{\lambda}_{LT,\theta,com} = \bar{\lambda}_{LT} \sqrt{\frac{k_{y,\theta,com}}{k_{E,\theta,com}}}$$

where $\bar{\lambda}_{LT}$ is the non-dimensional slenderness at room temperature, and with

$\alpha = \beta \varepsilon$ the imperfection factor;

β is the severity factor, to be chosen in order to ensure the appropriate safety level;

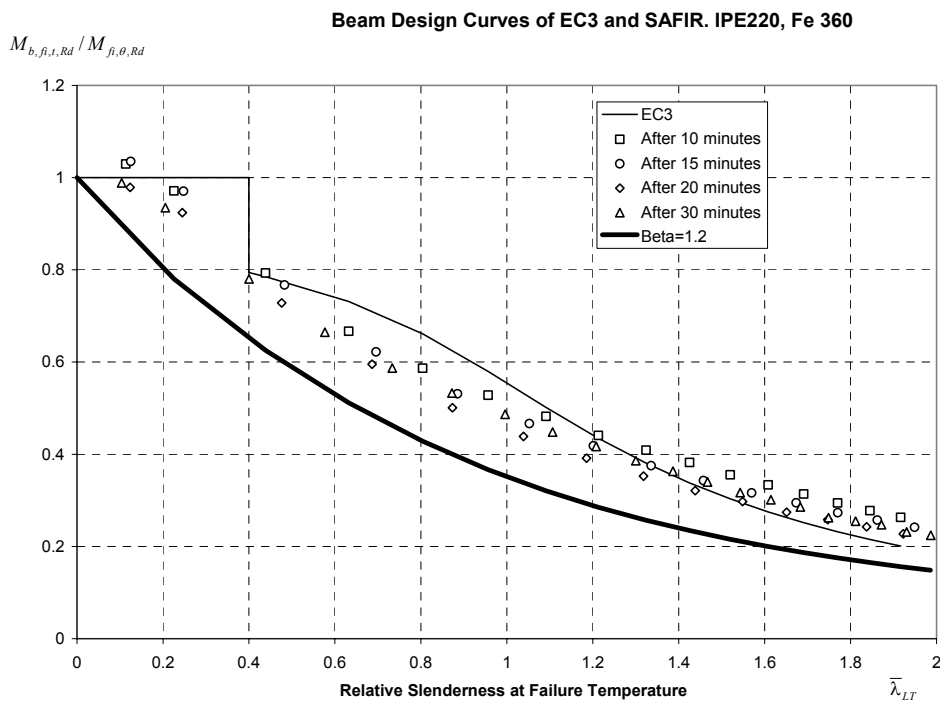
$\varepsilon = \sqrt{235/f_y}$, f_y in MPa is the yield strength.

Comparing equations (1) and (8) we can verify that with this new proposal we do not use the empirical constant 1.2 that is used as a correction factor in the proposal of the Eurocode 3.

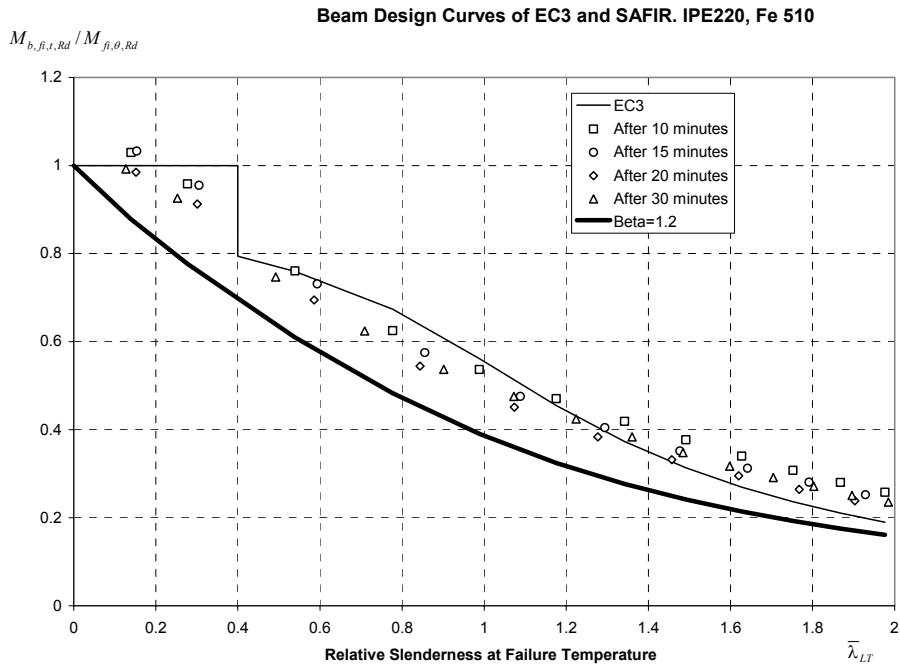
Equations (9) and (10) are in fact exactly the same as those defined at room temperature in Eurocode 3, Part 1-1 [1], except that the threshold limit of 0.20 for $\bar{\lambda}_{LT}$ does not appear in equation (10). The fact that the threshold limit does not appear changes the shape of the buckling curve. It differs from that at room temperature. The new curve starts at $\chi_{LT} = 1.0$ for $\bar{\lambda}_{LT} = 0.0$ but it decreases even for very low slenderness, instead of having a horizontal plateau up to $\bar{\lambda}_{LT} = 0.4$ (see Fig. 17 to Fig.19).

The lateral-torsional buckling curve varies with the yield strength due to the parameter ε that appears in the imperfection factor.

The beam design curve obtained with this new proposal using a severity factor $\beta = 1.2$ as in [6] is shown in Figure 17. This value of the severity factor seems to be very safe as it can be seen in that figure.



a) Fe 360 steel



b) Fe 510

Fig. 17 – Beam design curve obtained with Eurocode 3, SAFIR (after 10, 15, 20 and 30 minutes) and with the simply model of reference [6], with $\beta = 1.2$.

When comparing the simple model with experimental results for the fire resistance of axially-loaded members [9], Franssen et al. determined a severity factor with a value of 0.65 instead of 1.2. It must be mentioned that the value of 0.65 for the severity factor is the adopted value in the Belgium and French National Application Documents of Eurocode 3, Part 1-2, [10, 13].

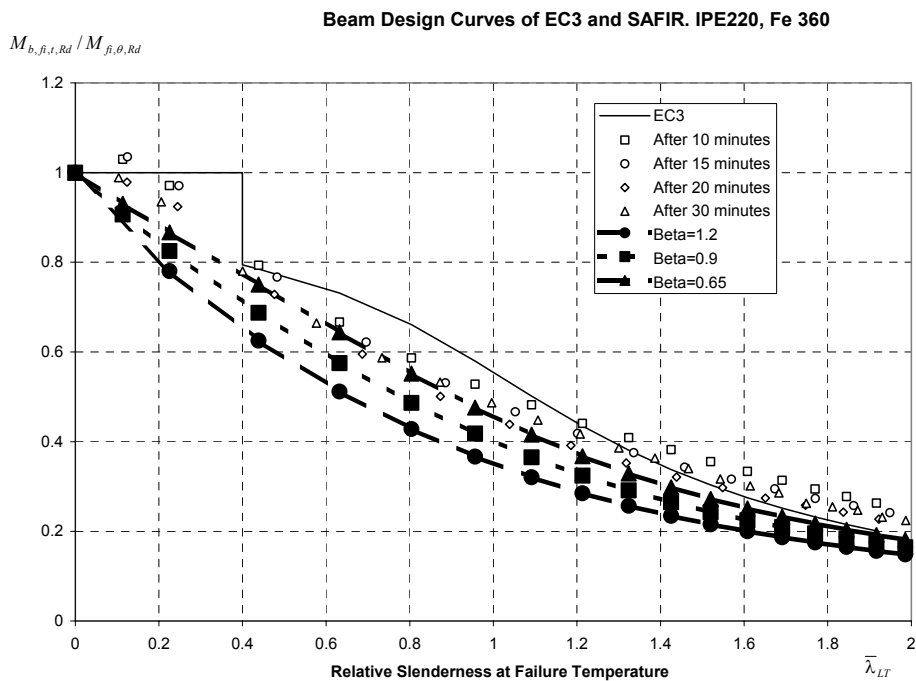
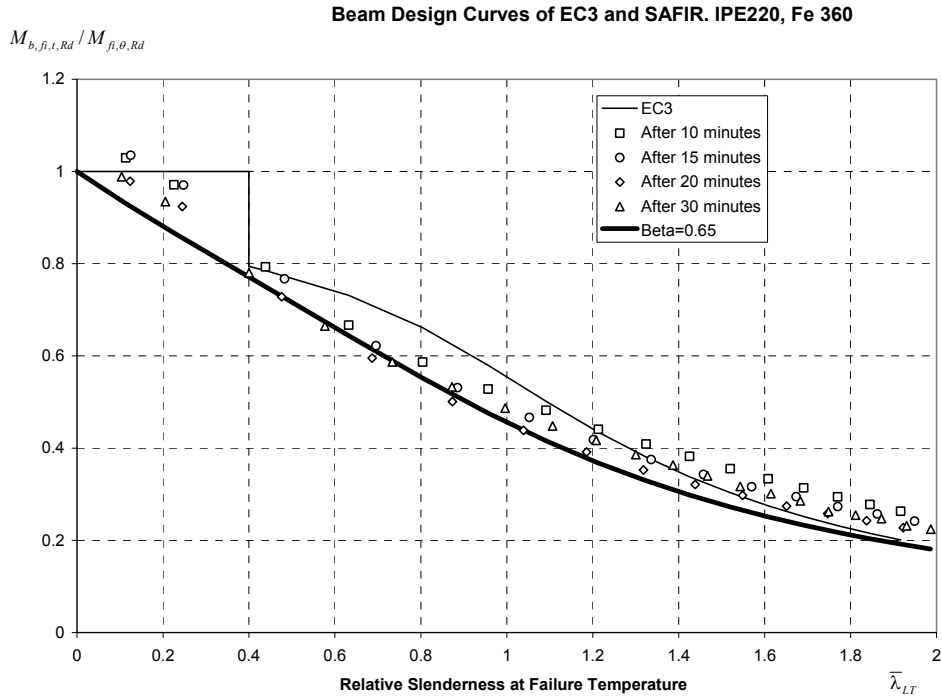


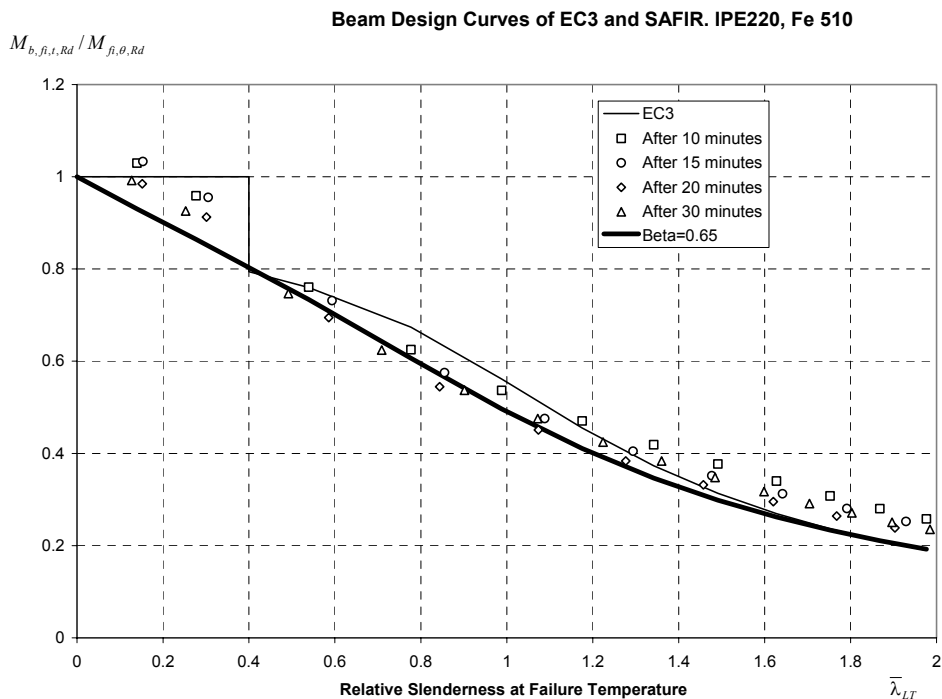
Fig. 18 – Beam design curve obtained with Eurocode 3, SAFIR (after 10, 15, 20 and 30 minutes) and with the simple model of reference [6].

Figure 18 shows the influence of the severity factor in the lateral-torsional buckling curve, for the Fe 360 steel. The values of 1.2, 0.9 and 0.65 have been used.

As the value of 0.65 for the severity factor gives safe results when compared with the SAFIR code, this value has been used in Figure 19 for the Fe 360 and Fe 510 steel.



a) Fe 360 steel



b) Fe 510

Fig. 19 – Beam design curve obtained with Eurocode 3, SAFIR (after 10, 15, 20 and 30 minutes) and with the simple model of reference [6], with $\beta = 0.65$.

As it can be seen in Figure 20, with this new proposal based on the results for axially-loaded columns [6], the beam design curve for lateral-torsional buckling now depends on the steel grade whereas the proposal of the Eurocode 3 does not. This dependence of the lateral buckling curve with the steel grade can be numerically supported with the results already shown in Figure 14.

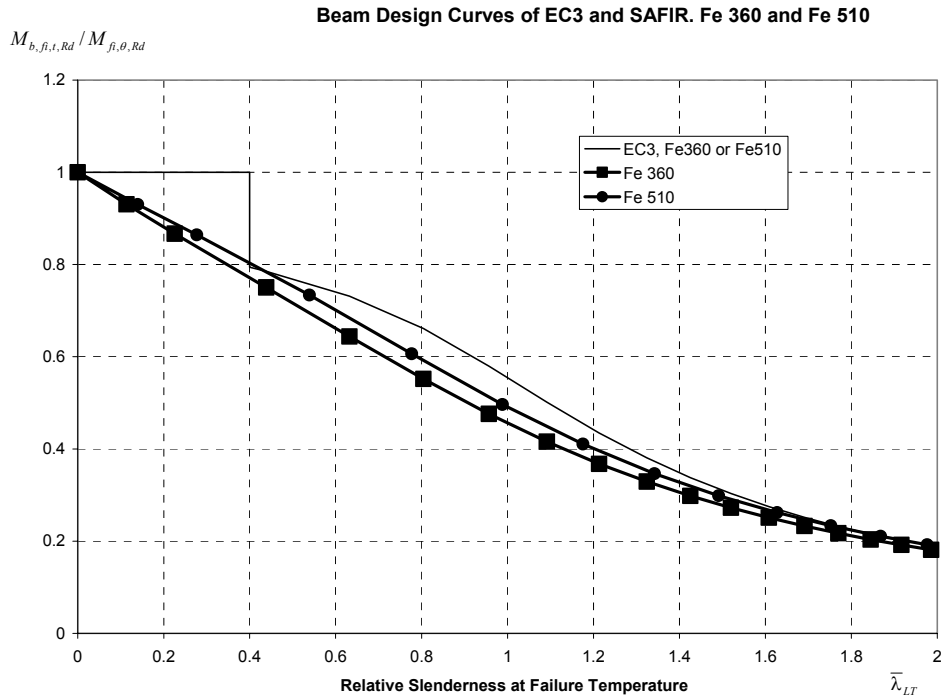


Fig. 20 – Beam design curves at elevated temperature obtained with the proposal of the Eurocode 3 and with the new proposal with $\beta = 0.65$.

4. CONCLUSIONS

The physical fact that Young's modulus decreases faster than the yield strength when the temperature increases, plus the fact that the stress-strain relationship at elevated temperature is not the same as at room temperature, produce a modification of the lateral-torsional buckling curve at elevated temperature. The horizontal plateau valid at 20 °C up to a non-dimensional slenderness of 0.4 vanishes in the case of elevated temperatures [6]. The simple models based on the lateral-torsional buckling curve that is valid at room temperature lead to a safety level that depends on the slenderness of the beam, the results being unsafe for intermediate length beams. It has been possible to make a new proposal of a lateral-torsional buckling curve for hot-rolled I-sections beams submitted to fire, based on the proposal suggested earlier [6] for axially-loaded hot-rolled H-sections submitted to fire. The beam design curve based on the reduction factor for lateral-torsional buckling in fire design situation and the non-dimensional slenderness evaluated at the ultimate temperature now depends on the steel grade, which is not the case in the Eurocode 3, Part 1-2.

It has been found that the same severity factor as the one used for the case of axially-loaded columns, i. e. $\beta = 0.65$ [9] could also be used here. This leads to the same philosophy as the one of Eurocode 3, i. e., to use the same formulas for the reduction factor for lateral-torsional buckling and for flexural buckling.

The severity factor β of the proposed simple calculation model has been established analysing only the behaviour of the IPE 220 profile. Further analysis of the numerical results should be done considering different steel I-sections.

It would also be worth to have results of well instrumented and carefully carried experimental tests to verify whether the present proposal can actually reproduce the test results and to fix definitely the value of the severity factor. As there is a low probability for the two structural imperfections, residual stresses and initial imperfection, to have simultaneously in a test the high amplitude assumed here in the numerical simulations, this could lead to the fact that the final adopted severity factor will be less severe than the one proposed in this paper.

ACKNOWLEDGEMENTS

Financial support from the Portuguese Foundation for Science and Technology, PRAXIS XXI research project PRAXIS/P/ECM/14176/1998 is acknowledged.

REFERENCES

- [1] Eurocode 3, Design of Steel Structures – Part 1.1. General rules and rules for buildings. Draft ENV 1993-1-1, Commission of the European Communities, Brussels, Belgium, 1992.
- [2] Eurocode 3, Design of Steel Structures – Part 1.2. General rules and rules. Structural fire design. Draft ENV 1993-1-2, Commission of the European Communities, Brussels, Belgium, 1995.
- [3] Jean-Marc Franssen, PROGRAM SAFIR, Ver. 1.3, User's Manual, Universite de Liege, Institut du Genie Civil, Service "Ponts et Charpentes", Dec. 1996.
- [4] D. Talamona, J. M. Franssen, J. B. Schleich, J. Kruppa, "Stability of Steel Columns in Case of Fire: Numerical Modelling", Journal of Structural Engineering, Vol. 123, No. 6, pp. 713-720, Jun. 1997.
- [5] Jean-Marc Franssen, "Contributions a la Modelisation des Incendies dans les Batiments et de Leurs Effects Sur les Structures", Thèse présentée en vue de l'obtention du grade d'Agrégé de l'Enseignement Supérieur, Année académique 1997-1998.
- [6] Jean-Marc Franssen, Jean-Baptiste Schleich & Louis-Guy Cajot, "A Simple Model for Fire Resistance of Axially-loaded Members According to Eurocode 3", Journal Construct. Steel Research, Vol. 35, pp. 49-69, 1995.
- [7] ECCS – EUROPEAN CONVENTION FOR CONSTRUCTIONAL STEELWORK, Technical Committee 8 – Structural Stability, Technical Working Group 8.2 – System, "Ultimate Limit State Calculation of Sway Frames With Rigid Joints", first edition, 1984.
- [8] ARBED. Sale Programme. Structural shapes. ARBED, Luxembourg, Octobre 1995.
- [9] Jean-Marc Franssen, Jean-Baptiste Schleich, Louis-Guy Cajot & Wenceslao Azpiazu "A Simple Model for Fire Resistance of Axially-loaded Members – Comparison with Experimental Results", Journal Construct. Steel Research, Vol. 37, pp. 175-204, 1996.
- [10] Eurocode 3 – Calcul des structures en acier – Partie 1-2: Règles générales – Calcul de comportement au feu, DAN belge, Juillet 1998.
- [11] Paulo M. M. Vila Real, Jean-Marc Franssen – "Lateral buckling of steel I beams at room temperature - Comparison between the EUROCODE 3 and the SAFIR code considering or not the residual stresses", internal report No. 99/01, Institute of Civil Engineering – Service Ponts et Charpents – of the University of Liege, Jan. 1999.
- [12] Eurocode 3 – Design of steel structures. Part 1 – General rules and rules for buildings. Background documentation. Cap. 5 document 5.03. Evolution of test results on beams with cross-sectional classes 1 – 3 in order to obtain strength functions and suitable model factors – October 1989.
- [13] Eurocode 3 - Calcul des structures en acier – Partie 1-2: Règles générales – Calcul de comportement au feu, Document D'Application Nationale française.
- [14] Franssen, J. M. – "Modélisation et influence des contraintes résiduelles dans les profils métalliques soumis à l'incendie", Construction Métallique, Vol. 3, pp. 35-42, 1989.
- [15] Franssen, J. M. – "The unloading of building materials submitted to fire", Fire Safety Journal, Vol. 16, pp. 213-227, 1990.
- [16] C. G. Bailey, I.W. Burgess & R. J. Plank, "The Lateral-torsional Buckling of Unrestrained Steel Beams in Fire", Journal Construct. Steel Research, Vol. 36, 1996, pp. 101-119.

